

Non-oxidative intercalation and exfoliation of graphite by Brønsted acids

Nina I. Kovtyukhova¹, Yuanxi Wang², Ayse Berkdemir², Rodolfo Cruz-Silva⁴, Mauricio Terrones², Vincent H. Crespi² and Thomas E. Mallouk^{1,2,3*}

Graphite intercalation compounds are formed by inserting guest molecules or ions between sp^2 -bonded carbon layers. These compounds are interesting as synthetic metals and as precursors to graphene. For many decades it has been thought that graphite intercalation must involve host-guest charge transfer, resulting in partial oxidation, reduction or covalent modification of the graphene sheets. Here, we revisit this concept and show that graphite can be reversibly intercalated by non-oxidizing Brønsted acids (phosphoric, sulfuric, dichloroacetic and alkylsulfonic acids). The products are mixtures of graphite and first-stage intercalation compounds. X-ray photoelectron and vibrational spectra indicate that the graphene layers are not oxidized or reduced in the intercalation process. These observations are supported by density functional theory calculations, which indicate a dipolar interaction between the guest molecules and the polarizable graphene sheets. The intercalated graphites readily exfoliate in dimethylformamide to give suspensions of crystalline single- and few-layer graphene sheets.

The intercalation of layered inorganic solids is an old topic of renewed interest as chemists seek to develop synthetic routes to single-layer graphene and other nanosheet materials. Graphite intercalation was first discovered in 1840 by Schafhäütl, who observed the formation of 'blue graphite' upon reaction with sulfuric acid and oxidizing agents¹. In 1855, Brodie found that a mixture of sulfuric acid and potassium chlorate or nitric acid produced a lamellar oxide of graphite². Since that time, numerous studies have shown that graphite can be intercalated by oxidizing or reducing agents^{3,4} and only one earlier report suggests the possibility of intercalation without adding an oxidizer⁵. Reactions of graphite with oxidizing acids or molecular oxidants such as Br_2 , AsF_5 or $FeCl_3$ result in intercalation compounds that contain both neutral and ionized guest species. The presence of both interlayer ions and neutral molecules in the intercalation compounds of graphite and other layered solids can be rationalized in terms of the energetics of intercalation^{6–8}. The endothermic opening of the galleries and ionization of the sheets is offset by the electron affinity of the guest and the lattice energy of the ionic product. Neutral molecules in the galleries further stabilize the compound by screening the repulsion between negatively charged guests. The dramatic increase in electronic conductivity relative to graphite and the blue-black colour of oxidatively intercalated graphite compounds reflect electron transfer between the carbon sheets and guest electron acceptors. However, over-oxidation results in the formation of covalent bonds, as in the case of graphite oxide or fluorides, with loss of conductivity^{9,10}. These highly oxidized graphite compounds can be exfoliated to form suspensions of individual sheets, which can then be chemically reduced to single-layer graphene¹¹. Single-sheet colloids can also be prepared from reductively intercalated graphite^{12,13}. However, in both cases the oxidation–reduction cycle creates defects in the sheets that destroy the spectacular electronic properties of single-layer graphene¹⁴.

We recently discovered that, under solvent-free conditions, Brønsted acids can intercalate layered boron nitride (h-BN)¹⁵. This was surprising, because h-BN had previously been intercalated only by the very strong oxidant $S_2O_6F_2$ (ref. 16). A detailed study of the h-BN compounds revealed that they were stabilized by host–guest acid–base interactions. Reasoning that graphene sheets can act as π -bases, we attempted the intercalation of graphite under similar conditions. We report here the synthesis of the resulting intercalation compounds, in which neutral graphene sheets encapsulate Brønsted acid molecules within the galleries. Once opened, the graphite layers are readily exfoliated to single- and few-layer graphene.

Results and discussion

Synthesis. Intercalation compounds were synthesized by mixing graphite powder with liquid acids (H_2SO_4 , H_3PO_4 , methanesulfonic ($MeSO_3H$), ethanesulfonic ($EtSO_3H$), 1-propanesulfonic ($n-PrSO_3H$) and dichloroacetic ($Cl_2CHCOOH$)) and heating the mixture to dryness. Although the reaction was typically carried out in air, control experiments (Supplementary Fig. 1b) established that the same products were formed when oxygen was rigorously excluded. After thermal drying of drop-cast films of graphite/acid suspensions, new phases were evident, together with residual graphite, in X-ray powder diffraction (XRD) patterns (Fig. 1a,b, Supplementary Fig. 1). Importantly, as in the h-BN/acid systems¹⁵, the intercalation reactions proceed only after drying of the acid suspensions. No intercalated phases were observed in liquid suspensions, even after several weeks, or in wet films. The intercalated phases that form when the samples are heated to dryness disappear upon exposure to water or the parent acid, and reappear upon drying, suggesting a reversible reaction in which no covalent guest–host bonds are formed.

The interlayer distances of the new phases were 7.32 ± 0.05 Å for graphite/ H_3PO_4 , 7.9 ± 0.1 Å for graphite/ H_2SO_4 , 10.9 ± 0.1 Å for graphite/ RSO_3H (R = methyl, ethyl, n -propyl) and 15.1 ± 0.1 Å for graphite/ $Cl_2CHCOOH$ (Fig. 1a,b, Supplementary Fig. 1).

¹Department of Chemistry, The Pennsylvania State University, University Park, Pennsylvania 16802, USA, ²Department of Physics, The Pennsylvania State University, University Park, Pennsylvania 16802, USA, ³Department of Biochemistry and Molecular Biology, The Pennsylvania State University, University Park, Pennsylvania 16802, USA, ⁴Research Center for Exotic Nanocarbons, Shinshu University, 4-17-1 Wakasato, Nagano 380-8553, Japan.

*e-mail: tem5@psu.edu

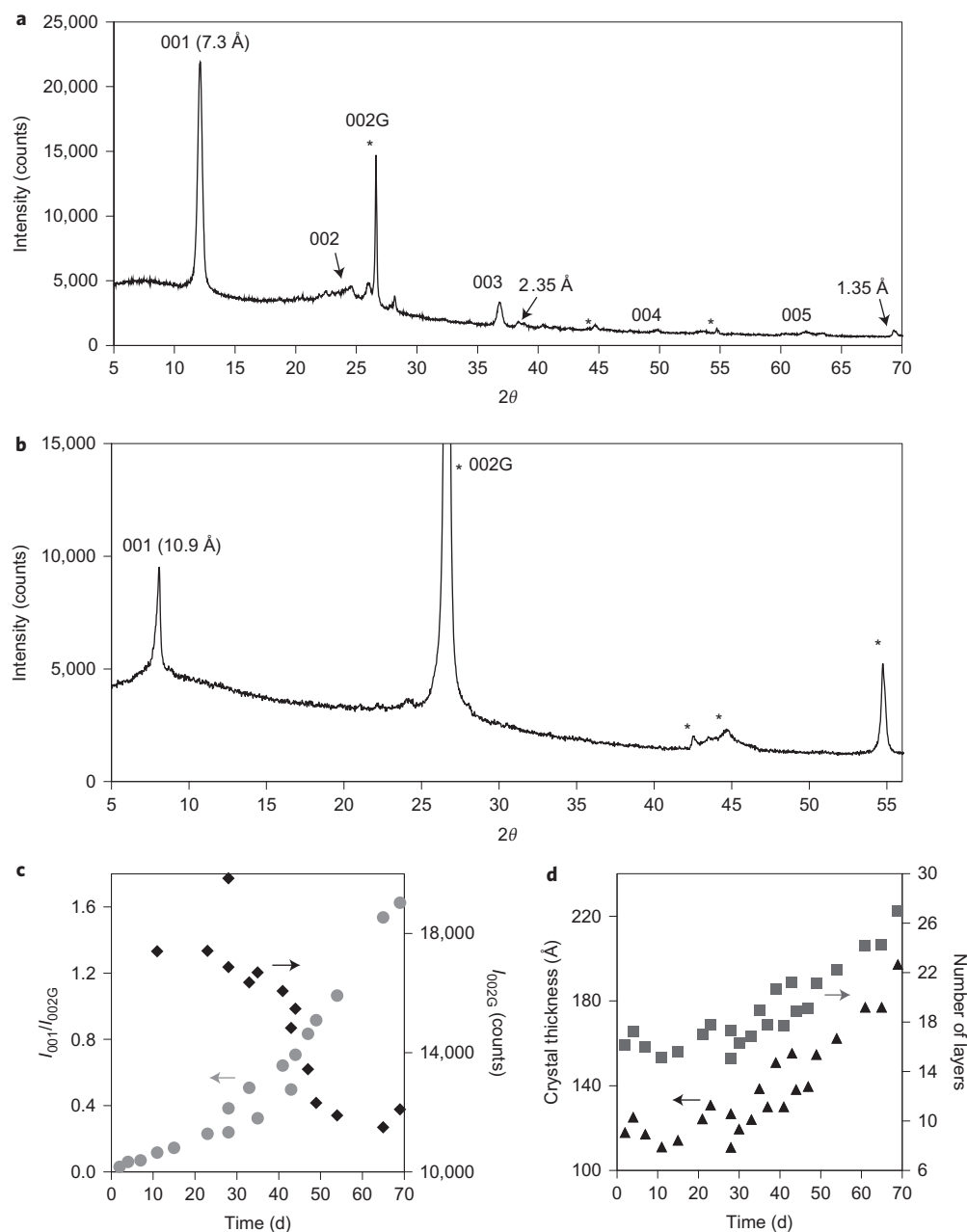


Figure 1 | X-ray diffraction data from dried cryo-milled graphite (CMG)/acid films showing the progress of the intercalation reactions. **a**, CMG/ H_3PO_4 (120 °C). **b**, CMG/ n -PrSO $_3$ H (90 °C). The $00l$ reflections of the intercalated phases are indicated (with arrows for weak reflections) as well as the d spacings of 001 and some un-indexed reflections. Graphite reflections are indicated with asterisks. 002G denotes the strong 002 reflection of graphite. **c**, Changes in relative intensity of the intercalated CMG/ H_3PO_4 phase (I_{001}/I_{002G}) and graphite (I_{002G}) reflections with time. **d**, Estimate of crystal thickness and number of graphene layers in the intercalated CMG/ H_3PO_4 phase versus time. The number of layers was obtained by dividing the thickness of the crystal grains (estimated from the Scherrer equation: $t = 0.94\lambda/\beta \cos \theta_{001}$; ref. 17) by d_{001} . Results shown in **c** and **d** were obtained in two parallel experiments conducted at 120 °C.

Comparison of the relative amounts of the intercalated phase shows that intercalation efficiency decreases in the order $\text{H}_3\text{PO}_4 > \text{Cl}_2\text{CHCOOH} > \text{EtSO}_3\text{H} > \text{PrSO}_3\text{H} > \text{MeSO}_3\text{H} \approx \text{H}_2\text{SO}_4$ (Supplementary Fig. 1). The dominant diffraction line in all cases was 001, although in some cases weaker 002–005 reflections could also be seen. The low intensity and breadth of higher-order $00l$ reflections, even in first-stage compounds, indicates poor ordering along the c axis. As the relative amount of first-stage graphite/ H_3PO_4 increased in mixed-phase samples, the 001 diffraction line narrowed, indicating that the crystalline domains of the intercalation compound grew in size. Figure 1c,d shows this correlation¹⁷.

For graphite/ H_3PO_4 and graphite/ H_2SO_4 , expansion of the interlayer galleries was 4.0–4.6 Å, as expected for a first-stage structure

with molecules intercalated between all the graphene planes. Similar layer expansion has been reported for intercalation with H_2SO_4 in the presence of oxidizing agents^{3,4}. However, first-stage graphite/ H_2SO_4 prepared from anhydrous acid remains black and no noticeable blue colour is observed.

In the intercalation compounds of n -alkylsulfonic acids (RSO_3H), the interlayer spacing does not depend on the length of the alkyl chain. This implies that the short chains (C1–C3) lie parallel to the graphene sheets. The d_{001} distances are ~ 7.6 Å larger than those of graphite, which is consistent with either the formation of stage-2 intercalation compounds or the presence of RSO_3H bilayers in the galleries of stage-1 intercalation compounds. The 15 Å diffraction line in the graphite/ Cl_2CHCOOH system

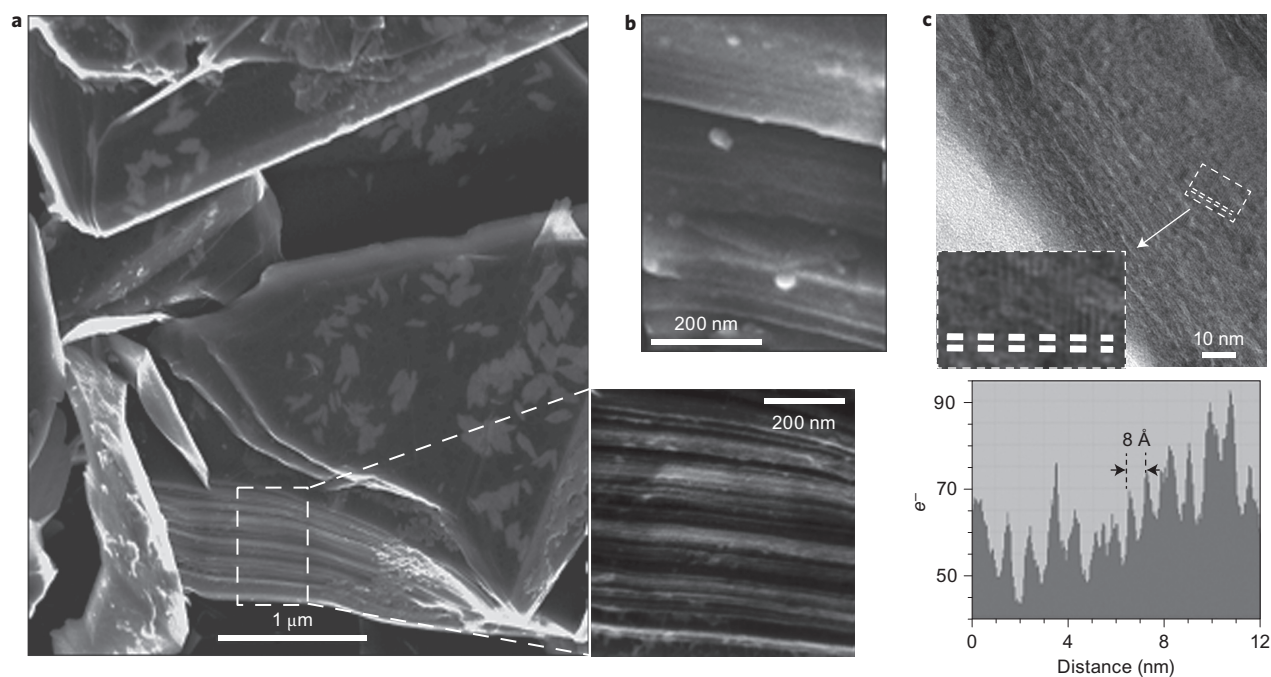


Figure 2 | Edge-on electron microscopy images showing the expansion of graphite particles upon intercalation. **a–c**, FESEM (**a,b**) and HRTEM (**c**) of intercalated graphite/*n*-PrSO₃H particles with a magnified view of the particle edge (**a**, inset), edges of the starting graphite crystals (**b**) and plan view of intercalated graphite/H₃PO₄ particles (**c**). Inset in **c**: expanded view and Moiré fringes. An image profile taken along the double dashed line in the inset shows the 8 Å spacing of Moiré fringes (bottom). The appearance of these fringes suggests that the sheets are slightly misoriented by the intercalation reaction.

suggests a higher-stage compound, or possibly a multilayer of acid molecules in the galleries.

Determining the stoichiometry of the intercalated phases was difficult because, for all acids studied, a significant amount of intact graphite remains, even when excess acid is used. X-ray photoelectron spectroscopy (XPS) and energy-dispersive spectroscopy (EDS) of graphite/H₃PO₄ gave measured C/P ratios in the range of 0.8–1.2. This low value suggests that some H₃PO₄ is adsorbed on the external surface of the graphite crystals. In the graphite/EtSO₃H system, however, the C/S ratio (measured by EDS) was in the range of 4–6 for specimen areas dominated by smaller particles. This is close to the composition of stage-1 graphite bisulfate, C₂₄⁺H₂SO₄[−](2H₂SO₄) (ref. 18), consistent with filling the entire volume of the galleries with H₂SO₄ molecules.

The crystallinity and particle size of the host material play an important role in intercalation reactions¹⁹. We therefore studied three types of graphite powder: natural graphite crystals (GAK-2), cryo-milled synthetic graphite (CMG) and spectroscopic graphite (SP-1) (Supplementary Fig. 2). The intercalation of van der Waals solids is known to proceed from the edges of the outermost layers inward, and successively into the bulk of the crystal^{20–22}. Thus, small crystallites give more rapid and complete intercalation. Indeed, EDS mapping of CMG/EtSO₃H confirms a higher sulfur and oxygen content in areas dominated by smaller crystals and by crystal edges (Supplementary Fig. 3). In the graphite/H₃PO₄ system, the relative amount of intercalated phase observed with CMG (crystal size of ~0.2–10 μm) was higher than with GAK-2 (~1–100 μm) or SP-1 (~1–200 μm) by factors of 10 and 30, respectively. Nevertheless, all three graphites showed the same expansion of the interlayer galleries in the intercalated phase. At the earliest stage of the reaction, the crystal thickness (in terms of the number of layers) did not noticeably change with time and remained in the range of 120 ± 10 Å (15–18 layers) (Fig. 1c,d). At this point, the increased amount of the intercalated phase was probably due to the growing number of small crystallites involved. After ~30 days, the thickness of the intercalated crystals began to increase almost

linearly with time, indicating that the intercalation of larger particles was considerably slower. These thicker crystals are probably of higher crystalline quality, judging from an appreciable decrease in the intensity of the residual 002 graphite reflection.

Electron micrographs of a graphite/*n*-PrSO₃H film (Fig. 2a) show that graphite particles delaminate upon reaction with the acid. The particles swell and split into 4- to 20-nm-thick slabs along their edges (Fig. 2a). The thickness of these slabs is of the order of the grain size inferred from XRD line widths (Fig. 1d). In contrast, the edges of the starting graphite crystals are relatively smooth and the lamellar slabs, which are discernible in electron micrographs, are much thicker and tightly packed within the 30- to 100-nm-thick crystals (Fig. 2b).

A plan-view high-resolution transmission electron microscopy (HRTEM) image of a graphite/H₃PO₄ particle (Fig. 2c) reveals parallel Moiré fringes spaced ~8 Å apart that orient approximately perpendicular to the edge of the particle (see inset). There are also random fringes that lie roughly parallel to the edges of the particles. These patterns may arise from displacement and misorientation of few-layer-thick neighbouring crystals of the intercalated phase.

X-ray photoelectron and vibrational spectra. Because phosphoric acid gave the highest yield of the intercalated phase, detailed spectroscopic and computational studies were carried out to characterize its intercalation compounds. XPS spectra (Fig. 3) show strong similarity between the starting graphite and intercalated phases. Notably, the C1s binding energy, which is sensitive to the oxidation and reduction of carbon, is the same within experimental error in graphite and graphite/H₃PO₄. However, the peak for the latter is much broader and has a shoulder on the high energy side (Fig. 3a,b). The broad major peak of the intercalated sample, fit tentatively to three components, suggests the presence of both electron-rich and electron-poor carbon in the intercalation compound. The relatively small differences between binding energies of pristine graphite and the new components (0.3–0.5 eV) does not support

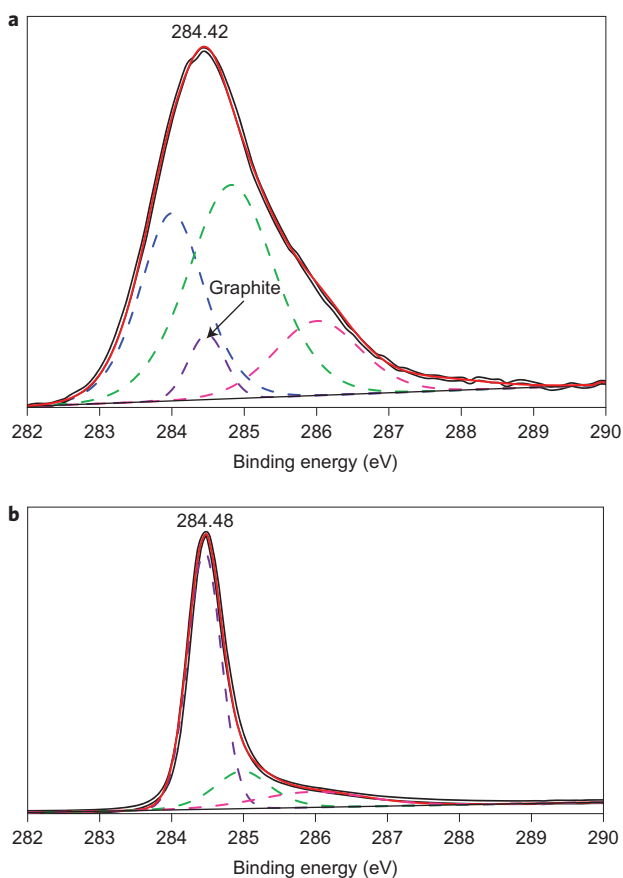


Figure 3 | XPS spectra show only small changes in electron density in the sp^2 -bonded carbon sheets upon intercalation with acids. a,b, C1s XPS spectra of a dry film of first-stage graphite/ H_3PO_4 (a) and starting graphite powder (b). All spectra were calibrated for $BE_{C1s} = 284.5.0$ eV. Compound black curves are experimental spectra, red curves are curve-fitting envelopes. The spectrum of the intercalated sample is dominated by electron-rich and electron-poor regions of the sheets (blue and green dashed curves, respectively), plus a smaller amount of residual graphite (purple dashed curve). The magenta dashed curve in both spectra represents an oxidized carbon component, probably at the edges of the crystals. BE, binding energy.

the formation of polar covalent bonds (for example, C–O) and can be explained (see below) in terms of dipolar interactions with the intercalated acid molecules. Calculated core level shifts from a simple structural model (Supplementary Fig. 8 and p. 6) were in the range of 0.09–0.17 eV, comparable to, but somewhat smaller than, the observed broadening of the C1s peak. In both the graphite spectrum and that of the intercalated sample, the high-energy component at ~ 286.2 eV can be attributed to oxidized carbon at the edges of the sheets.

The vibrational spectra of the intercalated graphite compounds (Supplementary Figs 4–6) are consistent with the small C1s binding energy shifts seen in XPS. The Raman G and D bands in graphite/ H_3PO_4 are very similar to those of graphite, implying that intercalation does not significantly disrupt the π -system by introducing defects (for example, sp^3 carbon atoms). Infrared spectra of acid-intercalated graphites show a decrease in the intensity of continuous absorption bands in the O–H stretching region, indicating that the continuous hydrogen-bonding network present in the liquid acids is disrupted in the intercalation compounds. Intercalated acid molecules are present in several chemical environments, which include donor/acceptor interactions with the π -system of the graphene sheets and weakly hydrogen-bonded molecular

clusters. A similar picture was observed for h-BN intercalation compounds with H_3PO_4 and H_2SO_4 (ref. 15).

Exfoliation of acid-intercalated graphite. An important consequence of graphite intercalation by neutral acids is the ease with which the sheets can be permanently delaminated to give single- or few-layer graphene. In this process, the intercalated acid is removed from the galleries and dissolves in the solvent used to exfoliate the crystals. To illustrate this property, the GAK-2/ H_3PO_4 and CMG/ H_3PO_4 intercalation compounds were dispersed in dimethylformamide (DMF). We obtained relatively stable light-grey solutions with some precipitated black particles, which are likely to be intact graphite. Atomic force microscopy (AFM) and TEM analysis reveal that exfoliation of CMG/ H_3PO_4 results in mostly relatively small (<100 nm– 2 μ m lateral dimensions) monolayer (2–3 Å high) and bilayer (4–6 Å high) graphene sheets (Fig. 4a–d, Supplementary Fig. 5). The monolayer sheets dominate the distribution, followed by bilayers, with much smaller amounts of few (3–9) layer sheets. GAK-2/ H_3PO_4 particles exfoliate to give both 1- to 3-layer small (<1 μ m) single-crystal graphene sheets (Fig. 4e,f, Supplementary Fig. 6) and many larger (2–8 μ m) sheets of relatively uniform thickness in the range 3–3.5 nm/9–11 layers. This is consistent with exfoliation of the intercalated phase to give predominantly monolayer graphene and the presence of a higher fraction of larger crystals in the natural graphite sample that are slower to intercalate (Supplementary Fig. 2). The starting graphite powders, dispersed in the same way, do not give appreciable amounts of single-layer sheets, although the CMG sample gave many small bilayers together with much thicker crystals (Supplementary Fig. 5). The sample of GAK-2 dispersed in DMF mainly consists of large sheets with thicknesses in the range of 2–9 nm and very few small 2- to 4-layer sheets (Supplementary Fig. 6). It appears that delamination of the graphite/acid particles into few-nanometre-thick slabs, which is accompanied by some displacement and misorientation in the crystal (Fig. 2a,c), facilitates exfoliation. It is important to note here that quantitative data on the exfoliation of small graphite/ H_3PO_4 particles involves some uncertainty. The distribution diagram in Fig. 4c was obtained by AFM analysis of 13 images (in total, 145 particles no smaller than 70 nm were measured). However, we always observed many graphene monolayer sheets smaller than 70 nm, as well as particle agglomerates, presumably formed on drying of the solutions, which could not be analysed by AFM.

Electronic structure calculations. Density functional theory (DFT) was used to constrain structural models of the intercalation compounds and to understand the interaction of acid molecules with the graphene sheets. To search for energetically favourable structures of intercalated H_3PO_4 , we prepared trial structures by inserting a single H_3PO_4 molecule into a 3×3 bilayer graphene supercell with the acid molecule at the midplane in random molecular orientations. The structure with two hydroxyl groups pointing towards the sheets (Fig. 5a) achieved the lowest energy. For a more precise estimate of the c -axis expansion, taking into account cross-sheet interactions, we extracted the gallery height ($h = 8.0$ Å) from the bilayer calculation and performed bulk calculations in a doubled cell containing two H_3PO_4 molecules and two layers of graphene (Fig. 5b), plus a series of bracketing calculations with gallery heights from 7.5 to 8.5 Å.

For graphite/methanesulfonic acid, the structure with the C–S bond of the acid parallel to the sheets and the hydroxyl group pointing toward the sheets achieved lowest energy. Two such bulk structures had c -axis periodicities close to the experimental value of 11 Å: stage-1 with a double layer of methanesulfonic acid in the gallery (Fig. 5c) and stage-2 with one layer of methanesulfonic acid in each gallery (Fig. 5d).

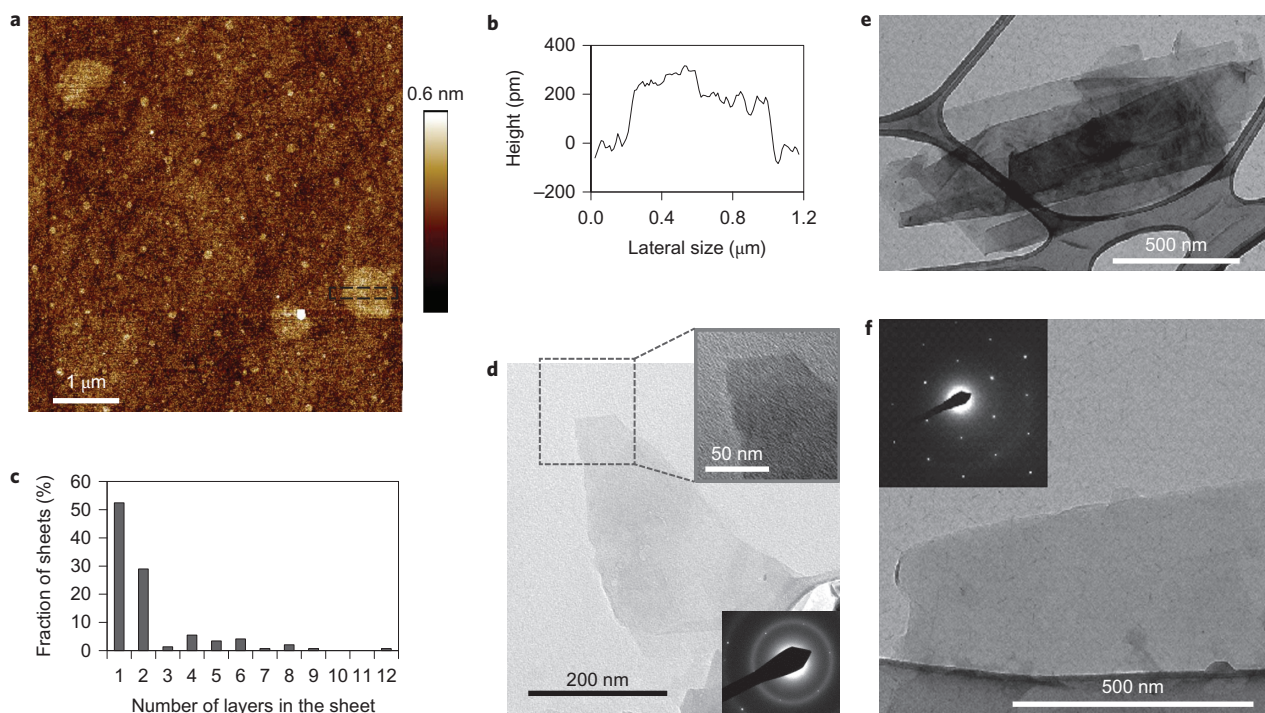


Figure 4 | Exfoliation of graphite is assisted by acid intercalation. a–f, AFM (**a,b**) and TEM (**d–f**) analysis of exfoliated graphite prepared by dispersion of CMG/ H_3PO_4 (**a–d**) and GAK-2/ H_3PO_4 (**e,f**) in DMF. **a**, Representative AFM height image of exfoliated CMG/ H_3PO_4 . **b**, The height of the sheets (marked by the black box in **a**) was measured by step analysis. **c**, Distribution of single- and few-layer graphene sheets in the decanted solution (145 sheets were measured). **d**, Folded monolayer graphene sheet on carbon film. Top inset: HRTEM image of sheet edges consistent with monolayer thickness. **e**, Thinning of GAK-2 crystals is evident from the contrast in the HRTEM images. Scrolling is also visible at the edges of sheets on the left side of the image. **f**, Trilayer single-crystal graphene sheet. Bottom inset in **d** and inset in **f**: selected-area electron diffraction patterns of the sheets.

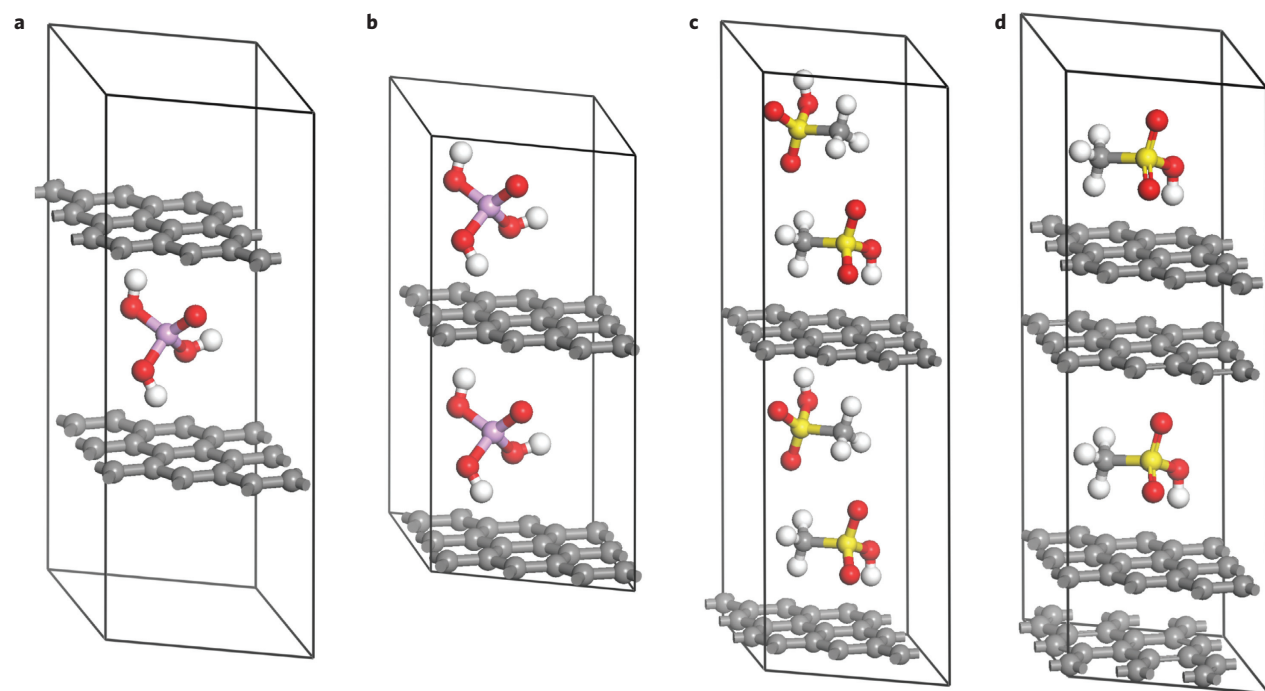


Figure 5 | Most energetically favourable structures of phosphoric acid-intercalated graphite from DFT calculations, showing the direct interaction of acidic OH hydrogen atoms with the carbon sheets. a, H_3PO_4 intercalated into bilayer graphene. **b**, Bulk graphite intercalation compound with H_3PO_4 . **c,d**, Stage-1 (**c**) and stage-2 (**d**) methanesulfonic acid intercalant geometries. Because methanesulfonic acid molecules have only one hydroxyl group, it is possible to form stage-1 structures with two layers of acid molecules per gallery (**c**), with the hydroxyl groups of molecules in each layer interacting with the neighbouring carbon sheet. A stage-2 structure (**d**) with a 3.35 Å shorter gallery height is also possible. Colour coding of atoms: carbon (grey), oxygen (red), hydrogen (white), phosphorus (pink), sulfur (yellow).

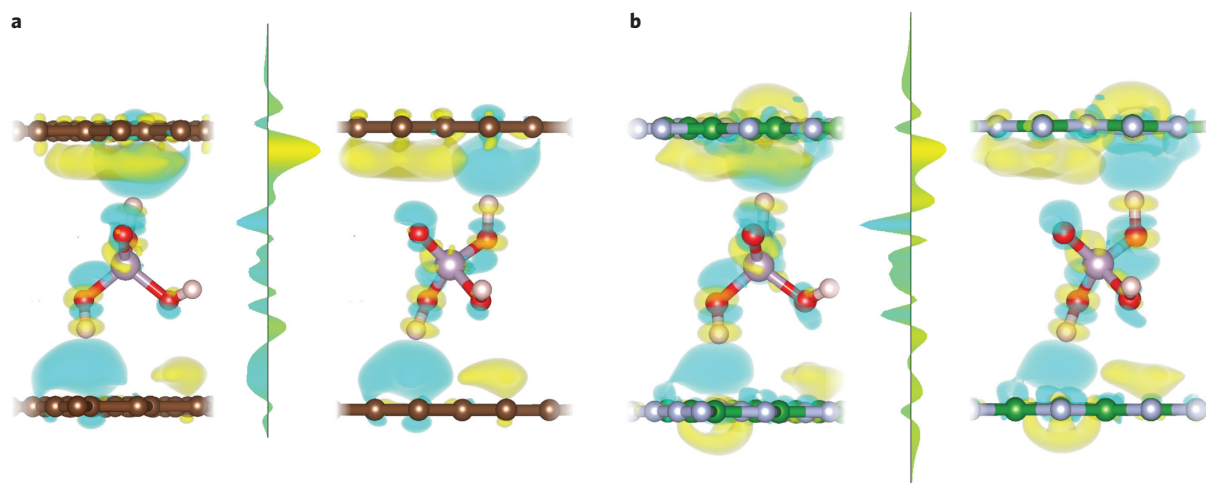


Figure 6 | Differential charge density map of H_3PO_4 -intercalated graphite and boron nitride. a,b, In both cases, H_3PO_4 -intercalated graphite (**a**) and h-BN (**b**), there are strong dipolar interactions between the guest molecules and the carbon or boron nitride sheets. Two views of each structure are shown. Cyan and yellow indicate charge accumulation and depletion, respectively. Colour coding of atoms: carbon (brown), oxygen (red), hydrogen (white), phosphorus (pink), boron (green), nitrogen (light grey). The differential charge density along the z axis, integrated over horizontal planes, is shown in the one-dimensional plots situated between the two views of each intercalation compound.

The shift in electron density upon intercalation can be used to discern the bonding interactions that stabilize the equilibrium geometry. We calculated the differential charge density by subtracting the charge density of separate systems containing isolated sheets or isolated acid molecules from the charge density of the combined relaxed system. Cyan and yellow isosurfaces in Fig. 6 depict regions of net electron accumulation or deficit upon intercalation. For comparison, both graphene and boron nitride intercalation compounds are shown with the same isosurface values. In addition to front and side views, we plot averages over horizontal slices at heights z , aligned to the adjacent views. The two partially positive hydrogen atoms closest to the sheets attract electron density from the adjacent layer (either nitrogen or the graphenic π -system). The charge accumulation integrated over the cyan cloud is $0.06e$ in both cases, indicating that metallic polarizability is not required to obtain a substantial polarization response in the layer. The oxygen atoms (especially the double-bonded one) of H_3PO_4 induce a local electron deficit in the sheets.

The appearance in the DFT calculations of regions in the graphene sheets showing charge accumulation or depletion is consistent with the broad C1s peak in the XPS of intercalated graphite (Fig. 3). Together, these data argue that a dipolar interaction with phosphoric acid molecules drives intercalation.

Conclusions

Experimentally established mechanisms of the redox-driven intercalation of van der Waals layered solids^{3,21,22} involve host-guest charge transfer, which facilitates opening of the outermost galleries. As the intercalation reaction proceeds, the galleries successively open in the bulk. The similarity of the intercalation reactions of h-BN (ref. 15) and graphite with Brønsted acids suggests a related mechanism for the non-oxidative intercalation reported here. The process is initiated by activation of the outermost host layers by acid-base rather than electron transfer reactions, and the guest molecule activity must exceed a threshold value for bulk intercalation to occur. XRD patterns show no evidence of intercalation in the presence of excess liquid acid; rather, heating to dryness is a necessary condition for the intercalation compounds to form, despite the fact that dehydration of the liquid acids is relatively fast and the acids maintain a constant composition thereafter¹⁵. It thus appears that non-oxidative intercalation can occur only under conditions where the hydrogen-bonding network of the

acid is disrupted by heating and partial evaporation at the graphite surface. The resulting acid molecules have higher thermodynamic activity than they do in the hydrogen-bonded liquid and are able to initiate the opening of the graphite galleries.

The ability to open the graphite galleries by chemical means, without strong oxidizing agents or apparent perturbation of the carbon sheets, enables the preparation of bulk quantities of single- or few-layer graphene by combining intercalation with dispersion in a polar solvent. It may be possible to obtain single-layer graphene exclusively through further optimization of the exfoliation conditions of these pre-intercalated materials. Many other van der Waals solids are of interest for electronic applications²³. These layered compounds also contain polarizable, Lewis basic sheets that may be amenable to intercalation by similar reactions. The success of this method at the pure-carbon and pure-BN ends of the BCN series suggests that layered sp^2 systems of intermediate composition²⁴ should also be amenable to gentle Brønsted acid intercalation. These possibilities will be explored in future experiments.

Methods

Materials. Natural graphite (GAK-2), cryo-milled synthetic graphite (CMG) and spectroscopic graphite (SP-1, Bay Carbon) powders were used without additional treatment. XRD, XPS and scanning electron microscopy (SEM) data obtained from the starting powders were consistent with a pure graphite phase composed of polydisperse (CMG from <0.2 to $10\ \mu\text{m}$; GAK-2 from <1 to $100\ \mu\text{m}$ and SP-1 from ~ 1 to $200\ \mu\text{m}$) good-quality crystals. Small amounts of surface C-O groups were found by XPS. All acids, H_2SO_4 - SO_3 (20%), H_3PO_4 (85%), $\text{CH}_3\text{SO}_3\text{H}$ (99.5%), $\text{C}_2\text{H}_5\text{SO}_3\text{H}$ (95%), $\text{C}_3\text{H}_7\text{SO}_3\text{H}$ ($\geq 99\%$) and Cl_2CHCOOH ($\geq 99\%$) were commercial products and were used as purchased.

Synthesis. Graphite powder (20 mg) was mixed with 0.05 ml acid and drop-cast on a glass slide. The mixture was dried in air or N_2 atmosphere at $25\ ^\circ\text{C}$ (Cl_2CHCOOH), 60 – $90\ ^\circ\text{C}$ (RSO_3H) and 120 – $125\ ^\circ\text{C}$ (H_3PO_4 and H_2SO_4). The drying temperature was chosen to be below the acid decomposition point but high enough to enable drying within a reasonable period of time. The reaction products were black powders, very hygroscopic in the case of H_3PO_4 and H_2SO_4 , but stable in air at the temperature of drying or under dry conditions at room temperature.

Exfoliation of the intercalated GAK-2/ H_3PO_4 and CMG/ H_3PO_4 was performed by dispersion of ~ 1 mg of the dry sample in 1 ml of DMF. The GAK-2/ H_3PO_4 suspension was sonicated for 30 min at ambient temperature (low-power sonication bath, Branson 2200). The CMG/ H_3PO_4 suspension was not sonicated but stirred for 22 h. The resulting light-grey solutions were decanted to separate larger black particles.

Characterization. The as-prepared films were characterized by XRD (Philips Empyrean, Cu-K α radiation), TEM (JEOL 1200 EXII, accelerating voltage

80–120 kV and JEOL 2010, source LaB₆, accelerating voltage 200 kV) and field-emission SEM (FESEM; FEI NanoSEM 630 FESEM, accelerating voltage 3 kV). XPS data were acquired with a Kratos Axis Ultra, using monochromatic Al-Kα X-rays. Analysis chamber pressures were in the mid-10⁻⁸ Torr range during measurements. The pass energy was set at 20 eV and the step size was 0.1 eV for high-resolution scans. XPS spectra were charge-referenced to C1s at 284.5 eV. Micro-Raman spectra were obtained with a Renishaw inVia confocal microscope-based Raman spectrometer with a laser excitation wavelength of 514.5 nm and a ~1-μm-diameter laser spot. Fourier transform infrared spectra (FTIR) were collected in transmission with a Hyperion 3000 FTIR microscope. The scan area was 0.1 × 0.1 mm². A thin sample layer was deposited on a Si(100) substrate, which was kept at the temperature of the synthesis to prevent water absorption during the analysis. AFM analysis was performed with a Bruker Icon microscope in PeakForce QNM imaging mode using single-crystal Si(100) substrates.

Computation of minimum energy structures. To find energetically favourable configurations of H₃PO₄-intercalated graphite we initially examined multiple possible configurations of a single H₃PO₄ molecule by inserting H₃PO₄ into an 8 × 8 pre-opened bilayer graphene supercell with random molecular orientations (12 Å vacuum was included above and below the bilayers). The molecules were placed at the midplane of the bilayer at random lateral positions and subsequently relaxed into a local minimum using the ReaxFF empirical force field²⁵. Unlike our previous study with h-BN intercalation¹⁵, H₃PO₄ molecules did not orient their hydroxyl groups towards the graphene sheets after relaxation. However, this appears to be a deficiency of the current parameterization of the empirical potential; when the six most energetically favourable ReaxFF-relaxed structures among 100 samples were optimized further within DFT with lateral sizes limited to 3 × 3, all the acid molecules oriented one hydroxyl group towards the nearest graphene layer. We therefore manually prepared an additional 3 × 3 supercell structure with the acid molecule orienting two hydroxyl groups towards the graphene layers and achieved the lowest energy after optimization (Fig. 5a).

For the graphite/methanesulfonic acid intercalation compound we optimized five trial structures within the DFT calculations. Three structures had the C–S bond of the acid molecule oriented parallel to the sheets and the molecule rotated about the C–S bond axis at three distinct angles 120° apart, and two structures had the C–S bond perpendicular to the sheets and the hydroxyl group manually oriented either away or toward the sheets. As expected, within each of the parallel and perpendicular groups, the most favourable structures were those with the hydroxyl group pointing vertically towards the sheets. The global winner had acid molecules lying parallel to the sheets, and was selected for further bulk relaxation, following the same procedure as for H₃PO₄ and examining several different intercalant geometries at stage-1 and stage-2. Details of the calculations are provided in the Supplementary Information, pp. 5–8.

Received 13 December 2013; accepted 31 July 2014;
published online 7 September 2014

References

- Schafhäutl, C. Ueber die Verbindungen des Kohlenstoffes mit Silicium, Eisen, und anderen Metallen, welche die verschiedenen Gattungen von Roheisen, Stahl und Schmiedeeisen bilden. *J. Prakt. Chem.* **21**, 129–157 (1840).
- Brodie, M. B.-C. Note sur un nouveau procédé pour la purification et la désagrégation du graphite. *Ann. Chim. Phys.* **45**, 351–353 (1855).
- Dresselhaus, M. S. & Dresselhaus, G. Intercalation compounds of graphite. *Adv. Phys.* **51**, 1–186 (2002).
- Levy, F. (ed.) *Intercalated Layered Materials* (D. Reidel, 1979).
- Moissette, A. *et al.* Spontaneous intercalation of sulfuric acid into graphite and synthesis of a new graphite–uranyl sulfate compound. *Mater. Sci. Forum* **91–93**, 95–99 (1992).
- Hofmann, U. & Rüdorff, W. The formation of salts from graphite by strong acids. *Trans. Faraday Soc.* **38**, 1017–1021 (1938).
- Schollhorn, R. Reversible topotactic redox reactions of solids by electron-ion transfer. *Angew. Chem. Int. Ed. Engl.* **19**, 983–1003 (1980).
- Bartlett, N. *et al.* Oxidative intercalation of graphite by fluoroanionic species—evidence for thermodynamic barrier. *Adv. Chem. Ser.* **226**, 391–402 (1990).
- Lerf, A., He, H., Forster, M. & Klinowski, J. Structure of graphite oxide revisited. *J. Phys. Chem. B* **102**, 4477–4482 (1998).
- Worsley, K. A. *et al.* Soluble graphene derived from graphite fluoride. *Chem. Phys. Lett.* **445**, 51–56 (2007).
- Zhu, Y. *et al.* Graphene and graphene oxide: synthesis, properties, and applications. *Adv. Mater.* **22**, 3906–3924 (2010).
- Viculis, L. M., Mack, J. J. & Kaner, R. B. A chemical route to carbon nanoscrolls. *Science* **299**, 1361 (2003).
- Zhang, Z. W. & Lerner, M. M. Preparation, characterization, and exfoliation of graphite perfluorooctanesulfonate. *Chem. Mater.* **8**, 257–263 (1996).
- Nicolosi, V., Chhowalla, M., Kanatzidis, M. G., Strano, M. S. & Coleman, J. N. Liquid exfoliation of layered materials. *Science* **340**, 1420 (2013).
- Kovtyukhova, N. I. *et al.* Reversible intercalation of hexagonal boron nitride with Bronsted acids. *J. Am. Chem. Soc.* **135**, 8372–8381 (2013).
- Shen, C. P. *et al.* Intercalation of hexagonal boron nitride by strong oxidizers and evidence for the metallic nature of the products. *J. Solid State Chem.* **147**, 74–81 (1999).
- Cullity, B. D. *Elements of X-Ray Diffraction* 284–285 (Addison-Wesley, 1978).
- Bottomley, M., Parry, G., Ubbelohde, A. & Young, D. Electrochemical preparation of salts from well-oriented graphite. *J. Chem. Soc.* 5674–5680 (1963).
- Hooley, J. S. Isotherms of metal chloride vapors on graphite. *Carbon* **11**, 225–236 (1973).
- Carr, K. E. Intercalation and oxidation effects on graphite of a mixture of sulphuric and nitric acids. *Carbon* **8**, 155–166 (1970).
- McKelvy, M. & Glaunsinger, W. Molecular intercalation reactions in lamellar compounds. *Annu. Rev. Phys. Chem.* **41**, 497–523 (1990).
- Wang, C., McKelvy, M. & Glaunsinger, W. Early events in intercalation reactions: the preintercalation state. *J. Phys. Chem.* **100**, 19218–19222 (1996).
- Butler, S. Z. *et al.* Progress, challenges, and opportunities in two-dimensional materials beyond graphene. *ACS Nano* **4**, 2898–2926 (2013).
- Muchharia, B. *et al.* Tunable electronics in large-area atomic layers of boron–nitrogen–carbon. *Nano Lett.* **13**, 3476–3481 (2013).
- Van Duin, A. C. T., Dasgupta, S., Lorant, F. & Goddard, W. A. III ReaxFF: a reactive force field for hydrocarbons. *J. Phys. Chem. A* **105**, 9396–9409 (2001).

Acknowledgements

Electron and atomic force microscopy, FTIR and XPS were conducted at the Materials Characterization Laboratory of the Pennsylvania State University. The authors thank T. Clark and V. Bojan for help with TEM and XPS analysis and A. van Duin for help in developing the ReaxFF parameterization for modelling of the H₃PO₄/graphite system. This work is supported by US Army Research Office MURI grant W911NF-11-1-0362.

Author contributions

N.I.K. designed and performed the experiments. Y.W. performed computer simulations. A.B. collected Raman spectra. R.C. prepared CMG. T.E.M., V.H.C., M.T., Y.W. and N.I.K. supervised the research and contributed to the interpretation of data and writing of the paper.

Additional information

Supplementary information is available in the [online version](#) of the paper. Reprints and permissions information is available online at www.nature.com/reprints. Correspondence and requests for materials should be addressed to T.E.M.

Competing financial interests

The authors declare no competing financial interests.